

Muthumanickam Andiyappan<sup>a</sup>, Subramanian Sundaramoorthy<sup>a</sup>, Prasanna Vidyasekar<sup>b</sup>, Natarajan Tirupattur Srinivasan<sup>c</sup>, Rama Shanker Verma<sup>b</sup>

<sup>a</sup>Department of Textile Technology, Anna University, Chennai, India

<sup>b</sup>Stem cell and Molecular Biology Laboratory, Department of Biotechnology, Indian Institute of Technology Madras, India

<sup>c</sup>Department of Physics, Indian Institute of Technology Madras, India

# Characterization of electrospun fibrous scaffold produced from Indian eri silk fibroin

A scaffold, synthesized from bio-degradable polymers and *Bombyx mori* silk fibroin in the form of films and fibrous assemblies, has been used as the bio-material for in-vivo applications. In the present work, the scaffold was prepared from the fibroin of Indian eri silk via the electrospinning method. The diameter of the fibre produced was in the range of 300 to 900 nm. The scaffold was subjected to ethanol treatment to improve its dimensional stability, as there was the problem of curling and shrinking when it was treated with solutions used for the cell culture. The scaffold was characterized for surface, thermal and tensile properties. The dimensional stability of the scaffold improved and the porosity reduced, due to the treatment of the scaffold with ethanol. The average failure stress of the raw and ethanol treated scaffold was 2.34 MPa and 4.91 MPa respectively and the mean strain was 13.63 % and 7.91 % respectively. Bone marrow stromal cells were isolated from the bone marrow of Swiss albino mice, and cultured on the ethanol treated electrospun fibrous scaffold. Scanning electron microscopy of the culture was carried out to evaluate the attachment and growth of cells on the scaffold at different incubation periods. Mouse bone marrow stromal cells adhered and grew on the electrospun fibrous scaffold prepared from eri silk fibroin, and the cell density increased with increasing incubation periods.

**Keywords:** Eri silk fibroin electro spun fibre; FTIR; TGA; SEM; Tissue engineering

## 1. Introduction

The scaffold for tissue engineering applications should support cell attachment, migration, cell-cell interaction and cell proliferation; be biocompatible; biodegrade at a controlled rate; provide structural support for cells and neo-tissue formed on the scaffold; and have versatile processing options to alter the structure and morphology related to tissue specific needs [1]. Poly L-lactic acid (PLA), poly glycolic acid (PGA), poly lactic-co-glycolic acid (PLGA), polycaprolactone (PCL) and *Bombyx mori* silk fibroin have been used as the scaffold for tissue engineering applications [1].

Silk is a natural protein fibre containing fibroin and sericin. The fibroin of *Bombyx mori* (BM) silk has been shown

to possess excellent physical and chemical properties for biomedical applications [2] and has been used in various fields, such as cosmetics, food additives and medical materials [3, 4]. Studies show that the cell attachment on BM silk films was found to be as high as for collagen films [5–9]. The silk films induced lower inflammatory response in in-vivo applications compared to traditional porcine-based wound dressings, collagen and PLA films [8, 10, 11]. Sericin is the second protein in the silk that acts as glue, holding the fibroin filaments. It carries an extremely high concentration of the amino acid serine, which ranges from 16 to 38 mol. % in the different sericine [12]. The sericin content in the silk filaments may induce undesirable immunological problems [13, 14] in in-vivo applications.

The rare wild species of silkworms, such as the Indian eri silk (*Samia cynthia ricini*), which is exclusive to certain regions of south east Asia, has a lower sericin content of 15.4 % compared to that of BM silk having 31.6 % [15]. Non-mulberry silk worms, such as *Philosamia ricini* (eri silk) are hardy, resistant to environmental stress, and less susceptible to diseases, compared to BM and other mulberry silk worms, due to the difference in the biochemical composition and immunochemical characteristics of fibroin heavy chain [16]. The eri silk has higher moisture absorption, compared to BM silk [17]. The higher hydrophilicity of the matrix has an important role in cell attachment. The amino acid composition of eri silk contains more alanine, aspartic acid and arginine compared to that of BM silk [17]. Higher aspartic acid and arginine can form the sequence Arg-Gly-Asp (RGD). The eri silk contains amino acids with positively charged chains, viz., arginine, histidine and lysine contents higher than those of BM silk. The material which contains the RGD sequence and amino acids with a positive charge, could favour cell attachment [18]. Hence, in this project, it is endeavoured to study the potential of using eri silk fibroin, after removing the sericin, for animal cell culture applications.

The scaffold in different structures such as films, braids and knits has been used for tissue engineering [19]. A silk fibroin nanofibrous mat has many favourable characteristics, such as high porosity, a wide range of pore size distribution, and high surface area-to-volume ratio, which are favourable parameters for cell attachment, growth, and proliferation [20]. Electrospinning offers good opportunity for manipulating the structural and mechanical properties, enabling use of silk fibroin fibrous assembly as a scaffold

for cell culture. Hence, in this project, the scaffold is produced from eri silk fibroin by means of the electrospinning process.

Adult mesenchymal stem cells (MSCs) are a safe and relatively non-controversial alternative to embryonic stem cells (ESCs), though they do not display as high a potency as the extremely effective and pluripotent ESCs. MSCs are multipotent and give rise to limited lineages; however, well established protocols make these cells a robust and useful choice for clinical applications [21]. Bone marrow stromal cells (BMSCs) have been successfully shown to give rise to bone, cartilage, and mesenchymal cells. The bone marrow is the tissue where hematopoiesis occurs in close contact with the stromal microenvironment, which supports hematopoietic stem cell growth and differentiation. Stromal fibroblasts are able to support hematopoiesis, and are capable of differentiating between osteogenic, chondrogenic and adipogenic lineages. In vitro, they form colony forming units-fibroblasts (CFU-f), which in turn, give rise to BMSCs and MSCs [22]. The present work explores the feasibility of using electrospun eri silk nanofibres as scaffold for in-vitro culture of mouse bone marrow stromal cells.

The tensile and in-vitro degradation of an electrospun fibrous mat produced from eri silk fibroin was studied earlier by Muthumanickam et al. [23]. In the present work, the scaffold was treated with ethanol to prevent the problem of curling and shrinking when treated with the solutions used for tissue culture. The following characteristics of the scaffolds were studied: (i) Tensile strength and strain, which is essential to withstand the strain during cell culture, (ii) Scanning electron microscope (SEM) image analysis to know the diameter and surface structure of the scaffold, (iii) Thermogram from thermogravimetric analyzer (TGA) to know the structural stability of the scaffold due to temperature, (iv) X-ray diffraction (XRD) study to understand the change in property with reference to the crystallinity of the scaffold due to ethanol treatment and (vi) a Fourier transform infra red spectroscopy (FTIR) study to know the presence of solvents used for the preparation of the polymer solution, and change in functional groups due to ethanol treatment. The biocompatibility and ability for cell culture was assessed by the in-vitro culture of the mouse bone marrow stromal cells on the scaffold.

## 2. Experimentals

### 2.1. Preparation of eri silk fibroin scaffold

The eri silk was obtained from the Central silk board, Bangalore, India. Eri silk was degummed by immersing it in the sodium carbonate solution, kept at 75 °C and at a pH level of 8.5–9.0, for 30 min, to remove the sericin content. A polymer solution was prepared from the fibroin of eri silk by dissolving it in 99% concentration of tri-fluoro acetic acid for 10 min. The fibrous scaffold was produced using the electro-spinning process. The concentration of the silk fibroin solution and the electro-spinning parameters were optimized, such that there was no spraying of the solution or bead formation. The parameters used for electro spinning were: voltage – 20 kV; distance between the syringe and collection plate – 15 cm; and silk fibroin solution – 13% concentration (w/v). Each sample was prepared from the polymer solution of 5 ml vol. The porosity of the scaffold was calculated using the following equation:

$$\text{Porosity \%} = \left[ 1 - \frac{\text{apparent density of scaffold}}{\text{bulk density of fibre}} \right] \times 100 \quad (1)$$

The apparent density is the ratio of the mass-to-volume of the scaffold. The bulk density of the silk fibroin is 1.25 g cm<sup>-3</sup> [17]. An SEM image (Fig. 1) was taken to assess the diameter of the fibre and appearance of the scaffold. The histogram was constructed from 100 measures of diameter taken randomly from the SEM picture.

### 2.2. Treatment of the scaffold with ethanol

The scaffold has the problem of curling and shrinking when treated with the solutions used for tissue culture. Amiraliyan et al. [24] treated the electrospun nanofibrous mat of BM silk with methanol and ethanol, to improve the structural stability and crystallinity. Hence, the eri silk fibroin scaffold was treated with ethanol at room temperature for 30 min to improve the dimensional stability. To assess the improvement in the dimensional stability of the scaffold due to ethanol treatment, the scaffold was treated with

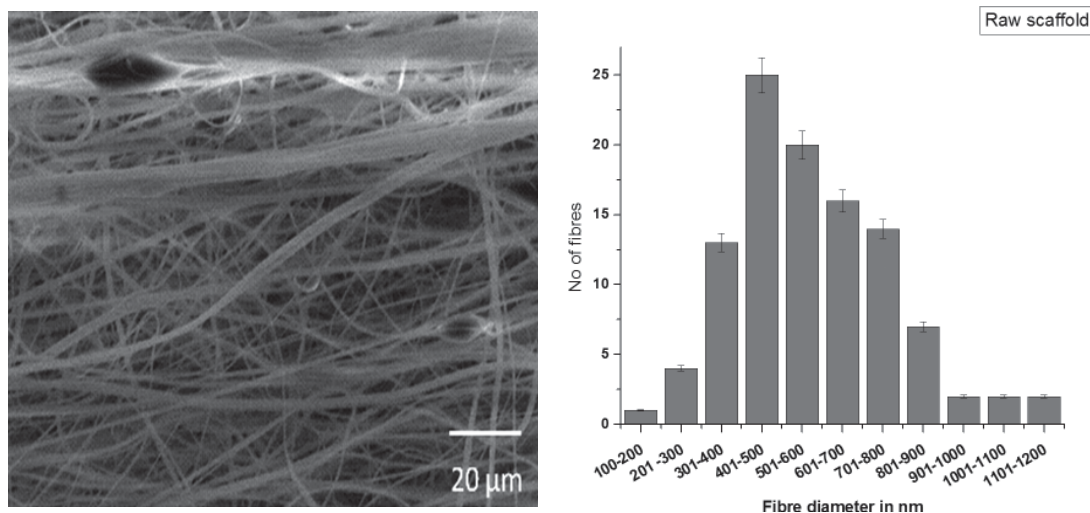


Fig. 1. SEM image of electrospun eri silk fibroin scaffold and histogram showing fibre diameter distribution.

Table 1. Dimensions and porosity of scaffolds.

S. No.	Material	Length (mm)	Width (mm)	Thickness (mm)	Area (mm <sup>2</sup> )	Weight (mg)	Porosity (%)
1	Raw scaffold	25	25	0.164	625	21	83.6
2	Raw scaffold in PBS	18	17	0.172	306	21	68.5
3	Scaffold treated with ethanol	20	20	0.164	400	21	74.4
4	Ethanol pre treated scaffold in PBS	20	20	0.159	400	21	73.5

phosphate buffer saline (PBS) before and after the ethanol treatment. The samples were conditioned at 37 °C and 65% relative humidity (RH) for one day. Table 1 shows the thickness and area of the scaffolds measured and porosity calculated, using Eq. (1).

### 2.3. Characterization of the scaffold for physical properties

The images of (i) the raw scaffold (without ethanol treatment); (ii) the raw scaffold in PBS, (iii) the scaffold treated with ethanol, and (iv) ethanol pretreated scaffold in PBS were obtained using an FEI Quanta 200 scanning electron microscope with a voltage of 15 kV to study the changes if any, in the surface characteristics, due to the ethanol and PBS treatment. The scaffolds were sputter coated with gold prior to taking the SEM images.

The raw and ethanol treated scaffolds were evaluated under XRD (Bruker) with Cu-K $\alpha$  radiation ( $\lambda = 1.54 \text{ \AA}$ ). The scanning speed was  $0.04^\circ \text{ s}^{-1}$  and the measurement range was 1 to 40° at 30 kV and 10 mA. The Gaussian peak fit method was used to measure the area of crystalline [25].

$$\text{Crystallinity \%} = \frac{\text{Area of crystalline}}{\text{Total area of crystalline}} \times 100 \quad (2)$$

The scaffold was tested for tensile properties under standard atmospheric conditions, using an Instron 3369 tensile strength tester. The scaffold was cut into a specimen size of 10 mm  $\times$  50 mm. Glue tapes were fixed at the top and bottom of the scaffold, where it is clamped on the jaw of the tester. The gauge length was maintained at 30 mm and the test speed was 20 mm min<sup>-1</sup>. The thickness of the scaffold was 0.16 mm  $\pm$  0.01 mm.

The FTIR spectra, in an attenuate total transmission mode, using a Bruker Spectrum, were recorded for the scaffold before and after the ethanol treatment, and also after autoclaving, to assess any change in the functional group. The scan range of the spectrum was set between 400 and 4000 cm<sup>-1</sup>. Thermal behaviour was assessed under a nitrogen atmosphere using TGA (Mettler Toledo, USA) in the temperature range of 50–700 °C at the rate of 20 K min<sup>-1</sup>.

### 2.4. Cell attachment and proliferation of bone marrow stromal cells on the scaffold

#### 2.4.1. Isolation of the bone marrow stromal cells from mice

Bone marrow was collected from two Swiss albino mice 6–8 weeks old, (Animal house, Kings' institute, Chennai, India) by flushing the femurs and tibias with the complete medium constituted of DMEM-F12 (Gibco, Invitrogen USA), 15% fetal bovine serum (FBS, Gibco), glutamine

2 mM (Gibco) and penicillin/streptomycin (50 U ml<sup>-1</sup> and 50 mg ml<sup>-1</sup> respectively, Gibco). The marrow was transferred to a 15 ml tube using a 1 ml pipette, where it was dispersed gently by the pipette and passed through a 70  $\mu\text{m}$  cell strainer. The tube was centrifuged at 1000 rpm for 5 min and the cells were re-suspended in 1 ml of fresh DMEM-F12. The cells were then plated into T75 and T25 flasks after taking a total cell count, using a haemocytometer. The medium was changed very gently, without disturbing the adherent cells, every 8 h for a period of 72 h. Then the cells were subjected to a medium change after every 36 h. A confluent culture was acquired by the end of two weeks.

#### 2.4.2. Cell culture and maintenance

Mouse bone marrow stromal cells were maintained in DMEM/F12 medium supplemented with 15% FBS, 2 mM L-glutamine, NEAA, 1% penicillin-streptomycin (Gibco), and 1 mM sodium pyruvate (Gibco). Cells were passaged at 90% confluency using 0.5% trypsin-EDTA (Gibco) and a cell scraper (Corning). Cells were maintained in a 37 °C, 5% CO<sub>2</sub> incubator (Thermo Scientific Corp.). Figure 2a–d shows the cells among the BMSC population that have MSC characteristics. Immunocytochemistry for FITC conjugated Sca-1, CD 44, CD 90 (BD Biosciences) and CD 29 (Santa Cruz Biotechnology Inc.), was carried out to establish MSC lineages in the total bone marrow population. Images were procured using a Nikon Eclipse Ti fluorescent microscope.

#### 2.4.3. Conditioning of the scaffold for cell culture

The silk scaffold was cut into strips of sizes (1.5  $\times$  1.5 cm) and sterilized by autoclaving (15 min, 121 °C, 1.034 bar) in a 50 ml tube. The tube was always opened under sterile conditions, and a pair of sterile tweezers was used to handle the strips of scaffold. The strips were transferred to 35 mm non-tissue culture grade sterile petri dishes. The dishes were incubated at 37 °C, 5% CO<sub>2</sub> overnight. The strips were then transferred to a fresh petri dish and allowed to dry inside the incubator kept at 37 °C, 5% CO<sub>2</sub>. The dried scaffold strips were then soaked in FBS for 3 h, and used for cell culture.

#### 2.4.4. Culturing BMSCs over the scaffold

The silk fibroin scaffold was submerged in DMEM-F12 prior to culturing. The BMSCs were counted and a total of  $0.5 \times 10^6$  million cells/mat (3–10 passages number) were seeded. The plates were kept undisturbed at room temperature for a few minutes, before transferring them to a 37 °C,

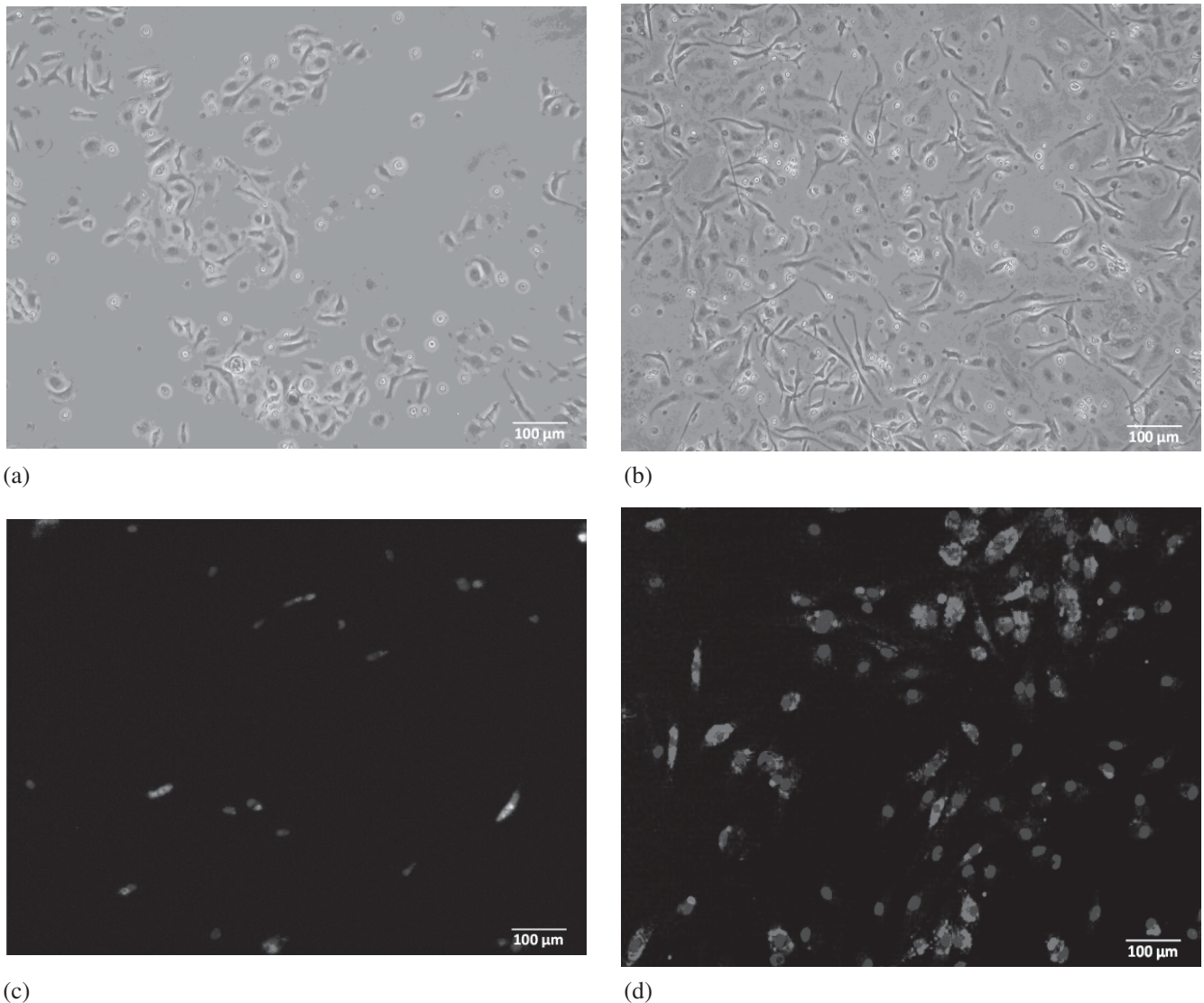


Fig. 2. (a) and (b) Bone marrow stromal cells isolated from Swiss albino mice with CFU-fs indicative of mesenchymal stem cells, and (c) and (d) immunocytochemistry of BMSCs showing positive cells for Sca-1 and Integrin beta 1 (CD 29), counter stained with Hoechst, a nuclear dye.

5% CO<sub>2</sub> incubator. The cells were allowed to adhere undisturbed for 48 h before any experiments.

#### 2.4.5. Cell morphology using SEM

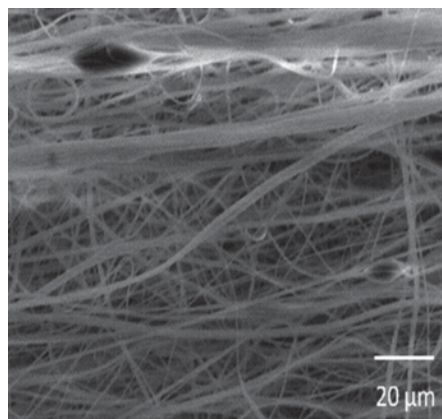
The cell-scaffold constructs were removed from the culture media after 3, 6 and 10 days. They were rinsed twice with PBS and then fixed with 4% glutaraldehyde for 45 min. The constructs were then subjected to a serial dilution of ethanol (40, 50, 60, 70, 80, 90 and 100%), for less than a minute in each dilution. The sample was rinsed twice with absolute alcohol. The rinsing was carried out gently and quickly, as the sample tends to suffer morphological changes during rinsing. The samples were then subjected to a quick drying process using a vacuum pump set at low pressure for less than two minutes. The cell-scaffold mats were visualized, using a FEI Quanta 200 SEM with SE (secondary electron) and BSE (backscattered electron) detectors. Bone marrow stromal cells seeded on eri silk scaffolds were observed for cell attachment and growth after the period of 3, 6 and 10 days of incubation from the SEM images.

### 3. Results and discussion

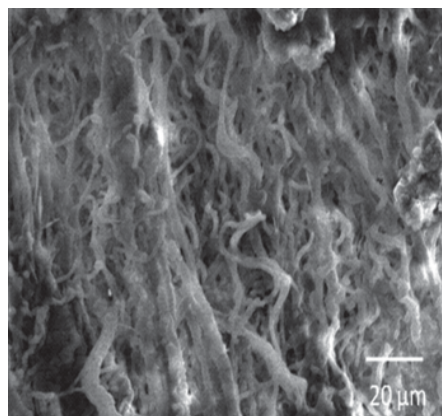
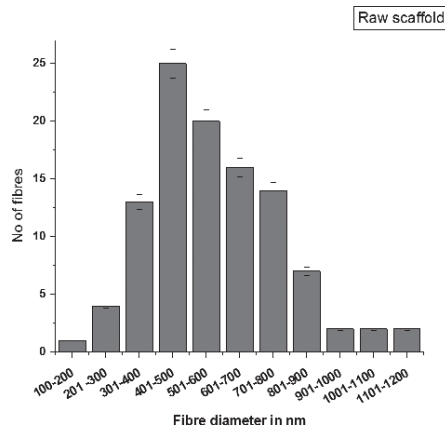
#### 3.1. Physical characteristics of the scaffold

##### 3.1.1. Structural stability

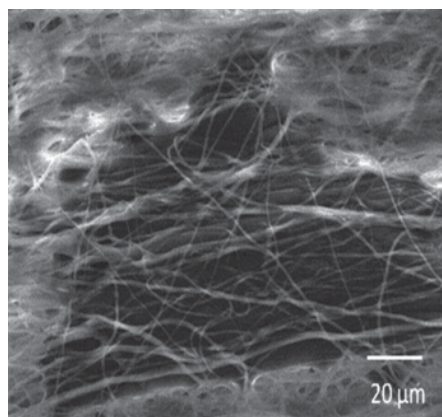
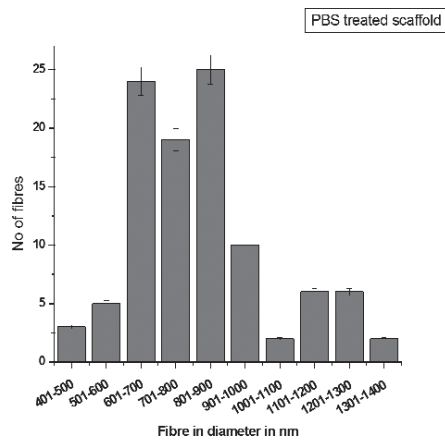
The dimensions and porosity of the raw, ethanol pretreated and PBS treated scaffolds are given in Table 1. It can be observed that the area of the scaffold reduces from 625 cm<sup>2</sup> to 410 cm<sup>2</sup> and the porosity reduces from 83.6% to 74.4%, due to treatment with ethanol. When the raw scaffold is directly treated with PBS, the reductions in the area and porosity are 51% and 18% respectively; but when the ethanol pre-treated scaffold was treated with PBS, the porosity reduces only by 1.2% and there is no reduction in the area. Whang et al. [26] found that 73.9% porosity was suitable for bone tissue engineering applications. The porosity of the scaffolds after treatment with ethanol is 73.5%, which is suitable for tissue engineering applications. The ethanol treatment improves the structural stability of the scaffold, in terms of shrinkage and curling.



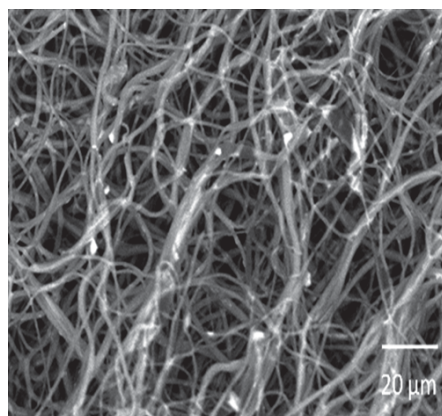
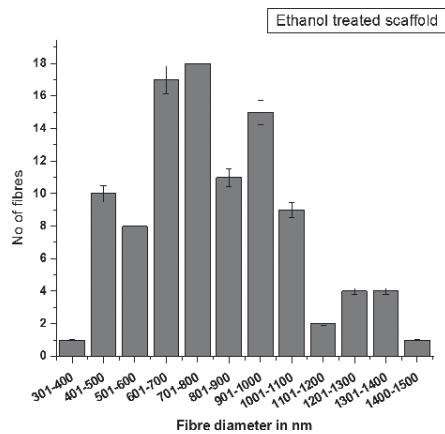
(a)



(b)



(c)



(d)

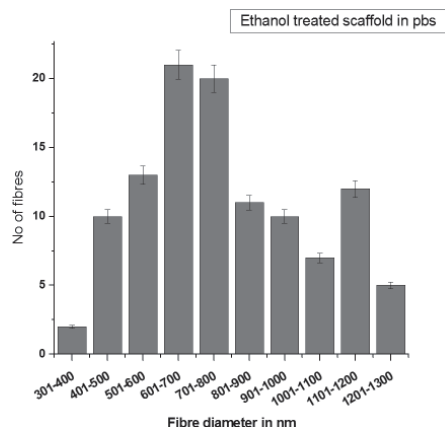


Fig. 3. SEM images and histograms showing fibre diameter distribution of (a) raw scaffold, (b) raw scaffold in PBS, (c) ethanol treated scaffold and (d) ethanol pretreated scaffold in PBS.

### 3.1.2. Surface characteristics using the SEM

Figure 3a shows that the diameter of the fibres is in the range between 300–900 nm, which is suitable for bone tissue engineering applications [27]. It can be observed from the SEM image in Fig. 3b that the surface is structurally deformed due to the treatment of the raw scaffold with PBS. Figure 3d shows that the surface is not deformed by PBS treatment, when it is pretreated with ethanol. It can also be seen from the Fig. 3c, that the surface of the scaffold is not deformed due to ethanol treatment. This shows that ethanol pretreatment helps to avoid the structural deformation of the scaffold while treating with PBS.

### 3.1.3. XRD analysis

The X-ray diffractograms Fig. 4a–c for degummed silk yarn and the ethanol treated electrospun scaffold, show the peaks prominently at  $2\theta = 11.20^\circ$ ,  $20.07^\circ$ ,  $28.82^\circ$  corresponding to  $\beta$ -sheet crystalline structure spacing 'd' of 7.9 Å, 4.48 Å and 3.2 Å respectively. However, the X-ray diffractogram Fig. 4b shows that raw electro spun fibre does not produce a prominent peak at  $2\theta = 20.07^\circ$  value, which corresponds to the crystalline structure of the ethanol treated scaffold [24, 28]. The crystallinity percentages of the pure eri silk fibroin (degummed silk), raw eri silknano fibre, and ethanol treated eri silk nano fibre, calculated using Eq. (2) are 50, 49.5 and 51 respectively. The result shows that the crystallinity of the eri silk fibroin is not altered due to the electrospinning process.

### 3.1.4. Tensile strength

Figure 5a and b show the tensile stress–strain curves of raw and ethanol treated scaffold samples. The result shows that the average breaking tenacity of raw and ethanol treated scaffold is 2.34 MPa and 4.91 MPa (with standard deviation of 1.78 and 1.81 Mpa) respectively, and the mean strain is 13.63% and 7.91% (with standard deviation of 3.38% and 2.79%) respectively. The ethanol treated scaffold has high-

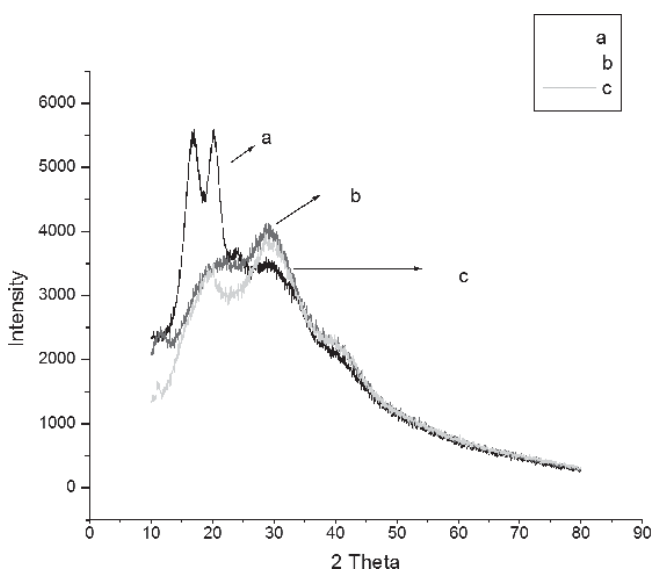
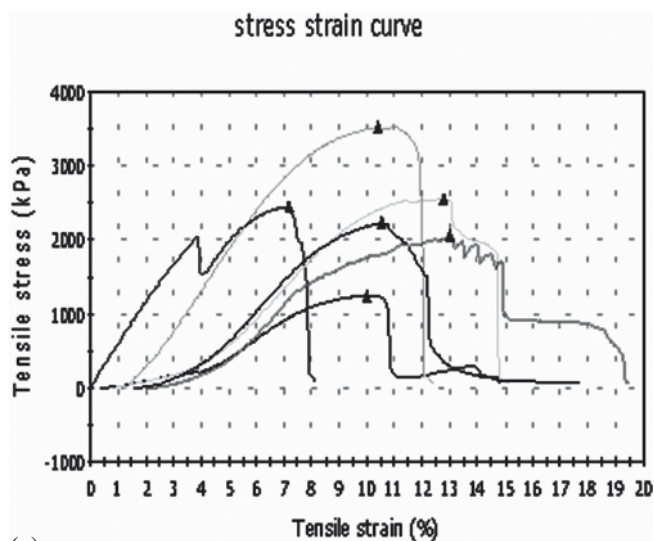


Fig. 4. X-ray diffractogram of (a) degummed eri silk yarn, (b) raw scaffold and (c) ethanol treated scaffold.

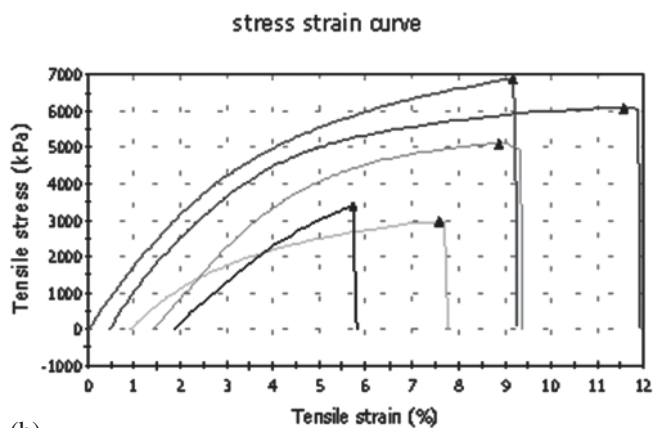
er tensile strength and lower elongation at break. The result matches with the finding of Amiraliyan [24] for the treatment of electrospun BM silk fibroin with methanol and ethanol. The increase in the tensile strength due to the ethanol treatment may be attributed to (i) an increase in the area of the fibre covered per unit area of the scaffold, due to a decrease in the area of the scaffold and (ii) an increase in the crystallinity of the fibre. The  $\beta$ -sheet crystalline structure and compactness of the scaffold due to the ethanol treatment, may be responsible for the decrease in the elongation at failure.

### 3.1.5. Thermogravimetric analysis

The TGA thermogram of the eri silk fibroin scaffolds is shown in Fig. 6a and b. The marginal initial loss in weight of both the raw scaffold and the ethanol treated eri silk fibroin scaffold, starts at  $100^\circ\text{C}$  due to the loss of the water content. Furthermore, it can be noted from Fig. 6a that the raw scaffold records a loss in weight for a second time in the range of  $200^\circ\text{C}$  to  $320^\circ\text{C}$  due to the breakage of the amide bonds in the silk fibroin, and ultimately decomposition starts above  $320^\circ\text{C}$ . The thermogram in Fig. 6b of the ethanol treated scaffold shows that the loss in weight during the second time happens in ranges from  $200^\circ\text{C}$  to  $350^\circ\text{C}$ ,



(a)



(b)

Fig. 5. Stress–strain curve for (a) raw and (b) ethanol treated scaffold (individual samples).

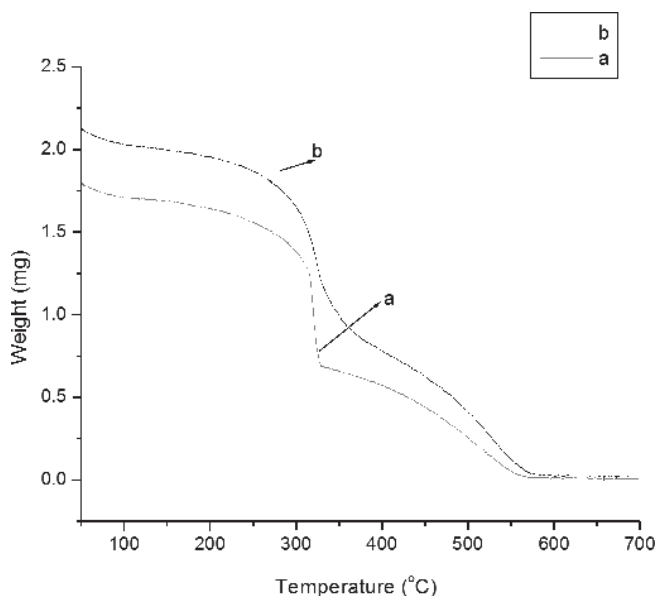


Fig. 6. Thermogram of (a) raw scaffold and (b) ethanol treated scaffold.

and it starts to decompose above 350 °C. This analysis shows that the ethanol-treated scaffold can withstand higher temperatures better than the untreated samples, since the ethanol treatment increases the crystallinity of the silk fibroin [28–30], and also the structural change to  $\beta$ -sheet form. The study also suggests that the ethanol-treated scaffold can be safely sterilized by autoclaving, since it withstands temperatures up to 350 °C, which is far above the autoclave sterilization temperature of 120 °C.

### 3.1.6. FTIR analysis

The assignment of various peaks of the FTIR spectra for the eri silk fibroin is given in Table 2. The presence of the secondary structures of protein is indicated by the following peaks in the FTIR spectrum: amide I (1600–1700  $\text{cm}^{-1}$ ) and amide II (1340–1440  $\text{cm}^{-1}$ ) [31, 32]. It can be noted from Fig. 7b that the stretch bands pertaining to tri-fluoro acetic acid (TFA) (1100–1200  $\text{cm}^{-1}$ ) used for preparing the fibroin solution, which may be allergen, are not found in the electro spun fibre [23]. It can be noted from Fig. 7a and b that the peak for amide II ( $\alpha$  helix structure) has shifted from 1357  $\text{cm}^{-1}$  to 1381  $\text{cm}^{-1}$ . Therefore, the presence of random  $\alpha$  helix has increased in the electrospun fibre of the eri silk fibroin, compared to that of the raw eri silk fibre. The spectra given in Fig. 7b and c show that the absorption peak for amide II has shifted from 1381  $\text{cm}^{-1}$  to 1375  $\text{cm}^{-1}$ , which indicates that the ethanol treated eri silk nano fibre has a higher content of  $\beta$ -sheet structure [24,

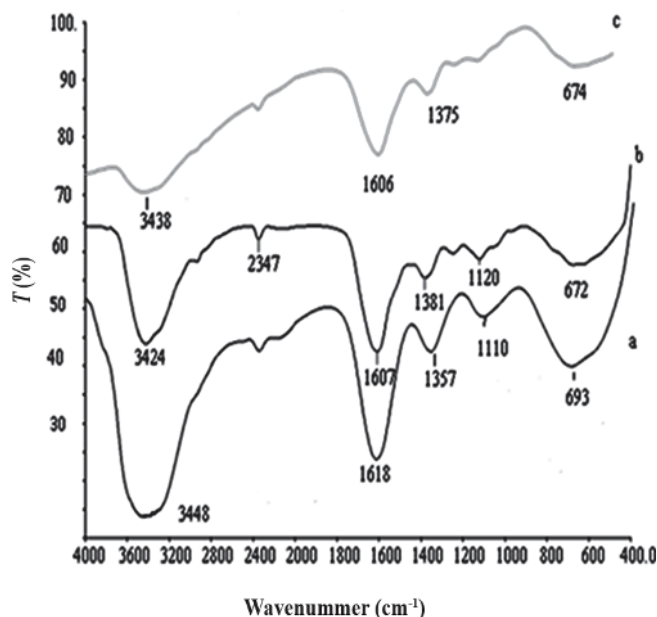


Fig. 7. FTIR spectra of (a) degummed eri silk yarn, (b) raw scaffold and (c) ethanol treated scaffold.

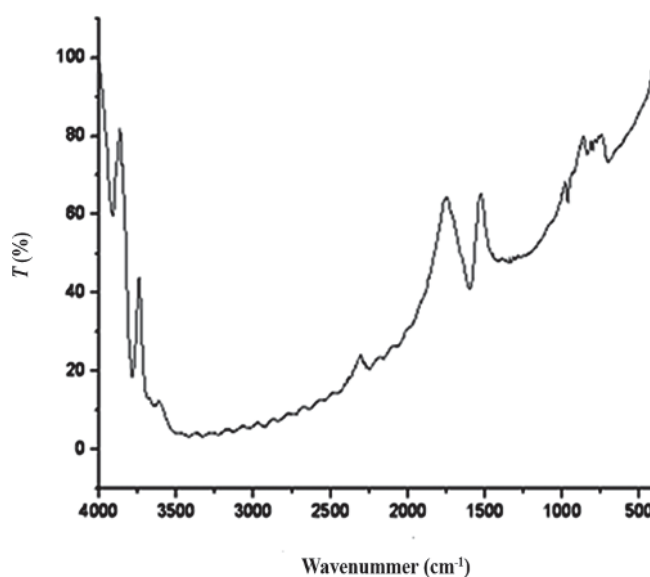


Fig. 8. FTIR spectrum of autoclaved eri silk scaffold.

30], and hence, it has better structural stability. The FTIR spectra (Fig. 8) of the autoclaved eri silk fibroin scaffold show peaks for amide I at 1599  $\text{cm}^{-1}$  and amide II at 1344  $\text{cm}^{-1}$ . The amide II shifted from 1381 to 1344  $\text{cm}^{-1}$ , which indicates that the autoclaved eri silk scaffold has more structural stability than the non-autoclaved scaffold.

Table 2. Wave number at FTIR spectra related to the elements of eri silk.

Materials	Amide I (wave number ( $\text{cm}^{-1}$ ))	Amide II (wave number ( $\text{cm}^{-1}$ ))
Raw eri silk	1618	1357
Electrospun eri silk fibre	1607	1381
Ethanol pretreated electrospun eri silk fibre	1606	1375
Auto claved eri silk fibre	1599	1344

### 3.2. Bone marrow stromal cell attachment on the scaffold

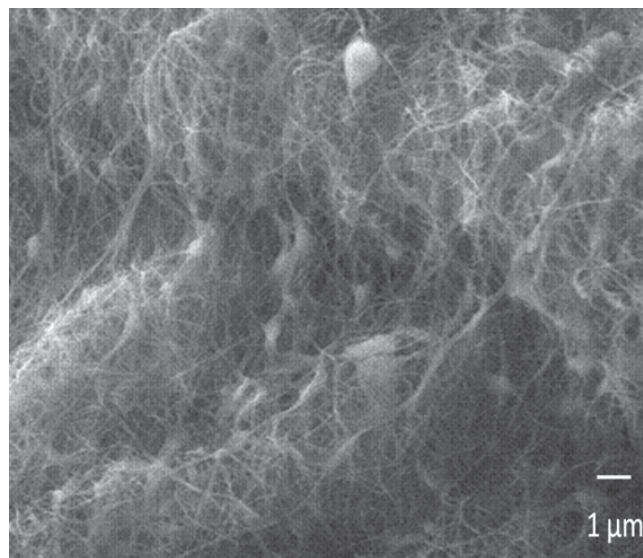
The BMSC attachment on the scaffold for different incubation periods is shown in Fig. 9a–c. The cell attachment on the scaffold is visible in Fig. 9a. The electro spun fibrous scaffold provides nano-scale contours, that may be responsible for the altered morphology, as it makes unique surfaces of the cell available for interaction with the neighbouring cells, unlike the 2-dimensional culture on conventional surfaces. The cell density visibly increases as the incubation period increases (day 6, day 10). Eri silk fibroin contains (Arg- Gly- Asp) RGD sequences in its molecules, and contains more amino acids with positive charge [17, 18, 33] which favour cell attachment and cell growth. The appearance and shape of the cells on the scaffolds also change with the periods of incubation, with cell colonies shifting from rotund masses to evenly spread mat like structures. These observations suggest, that electrospun eri silk fibroin mats are suitable as scaffolds for 3D tissue engineering applications involving BMSCs. This technology can be used to deliver in-vivo, specific cell types that have differentiated from the BMSCs grown in-vitro.

All procedures, approved by the Institutional Animal Ethics Committee (IIT Madras, India) and the Committee for the Purpose of Control and Supervision of Experiments on Animals, Government of India, were performed under the Rule 5(a) of the Breeding and Experiments on Animals (Control and Supervision) Rules (1998). All the animals used for the experiments were killed by cervical dislocation.

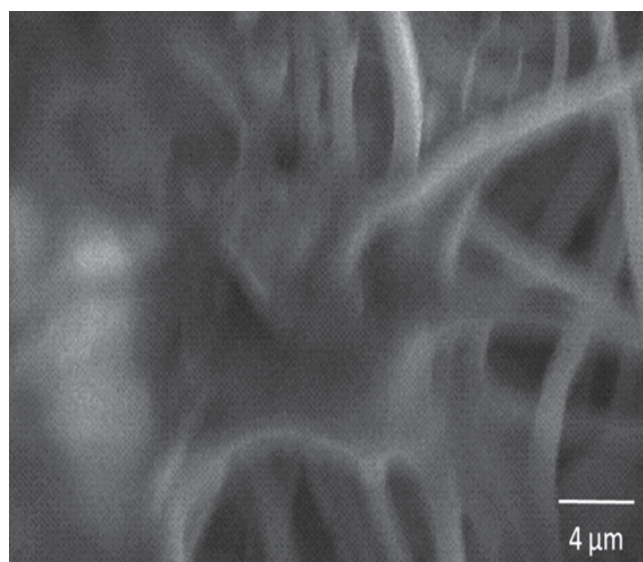
### 4. Conclusions

The following conclusions are drawn from this study:

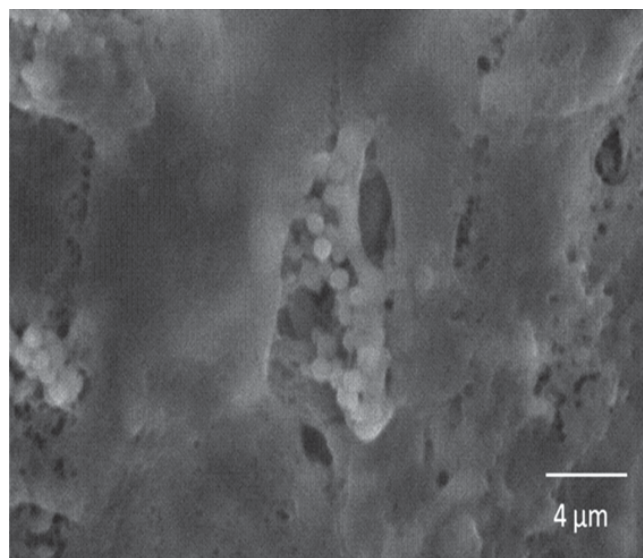
1. Fibrous scaffold can be prepared from eri silk fibroin by means of the electrospinning method with suitable process parameters. The diameter of the fibres is in the range of 300–900 nm.
2. Ethanol treatment improves the tensile strength of the scaffold. The average failure stresses of the raw and ethanol treated scaffold were 2.34 MPa and 4.91 MPa respectively, and the mean strains were 13.63% and 7.91% respectively.
3. The XRD analysis showed that the crystallinity of the eri silk fibroin is not altered due to the electrospinning process and ethanol treatment of the scaffold.
4. The SEM images showed that the ethanol treated scaffold and ethanol pretreated scaffold in PBS have more surface structural stability than the raw scaffold treated with PBS.
5. The TGA thermogram showed that the thermal stability of the ethanol treated scaffold is better than that of the raw scaffold. The decomposition temperature of both the scaffolds (above 320 °C) is higher than the temperature required for autoclaving (120 °C). The FTIR spectra showed that the structural stability of the scaffold increases due to treatment with ethanol.
6. The mouse bone marrow stromal cells adhered and grew on the electrospun fibrous scaffold prepared from the eri silk fibroin, and the cell density increases with increasing incubation periods.



(a)



(b)



(c)

Fig. 9. Mouse bone marrow cell attachment and growth at incubation period of (a) 3 days, (b) 6 days and (c) 10 days on the scaffold.

Part of this work is supported by the grant from DST (SR/SO/BB-07/2009).



## References

- [1] Y.-Z. Wang, H.-J. Kim, G. Vunjak-Novakovic, D.L. Kaplan: *Biomaterials* 27 (2006) 6064. PMID:16890988; DOI:10.1016/j.biomaterials.2006.07.008
- [2] W.H. Park, W.S. Ha, H. Ito, T. Miyamoto, H. Inagaki, Y. Noishiki: *Fibers and Polym.* 2 (2001) 58. DOI:10.1007/BF02875259
- [3] S. Sukigara, M. Gandhi, J. Ayutsede, M. Micklus, F. Ko: *Polymer* 44 (2003) 5721. DOI:10.1016/S0032-3861(03)00532-9
- [4] M.K. Sah, K. Pramanik: *Int. J. Environmental Sci. Developm.* 1(5) (2010) 404.
- [5] M. Santin, A. Motta, G. Freddi, M. Cannas: *J. Biomed. Mater. Res.* 46 (1999) 382. DOI:10.1002/(SICI)1097-4636(19990905)46:3<382::AID-JBM11>3.0.CO;2-R
- [6] N. Minoura, S. Aiba, Y. Gotoh, M. Tsukada, Y. Imai: *J. Biomed. Mater. Res.* 29(10) (1995) 1215. PMID:8557723; DOI:10.1002/jbm.820291008
- [7] N. Minoura, S. Aiba, M. Higuchi, Y. Gotoh, M. Tsukada, Y. Imai: *Biochem. Biophys. Res. Comm.* 208(2) (1995) 511. PMID:7695601; DOI:10.1006/bbrc.1995.1368
- [8] C. Vepari, D.L. Kaplan: *Prog. Polymer Sci.* 32 (2007) 991. PMID:19543442; DOI:10.1016/j.progpolymsci.2007.05.013
- [9] K. Inouye, M. Kurokawa, S. Nishikawa, M. Tsukada: *J. Biochem. Biophys. Methods*, 37(3) (1998) 159. DOI:10.1016/S0165-022X(98)00024-4
- [10] A. Sugihara, K. Sugiura, H. Morita, T. Ninagawa, K. Tubouchi R. Tobe: *Proc. Soc. Exp. Bio. Med.* 225(1) (2000) 58. DOI:10.1046/j.1525-1373.2000.22507.x
- [11] L. Meinel, S. Hofmann, V. Karageorgiou, C. Kirker-Head, J. McCool, G. Gronowicz: *Biomaterials* 26(2) (2005) 147. PMID:15207461; DOI:10.1016/j.biomaterials.2004.02.047
- [12] G. Freddi, R. Mossott, R. Innocenti: *J. Biotech.* 106 (2003) 101. DOI:10.1016/j.jbiotec.2003.09.006
- [13] L. Meinel, S. Hofmann, V. Karageorgiou, C. Kirker-Head, J. McCool, G. Gronowicz: *Biomaterials* 26(2) (2005)147. PMID:15207461; DOI:10.1016/j.biomaterials.2004.02.047
- [14] M. Santin, A. Motta, G. Freddi, M. Cannas: *J. Biomed. Mater. Res.* 46 (1999) 382. DOI:10.1002/(SICI)1097-4636(19990905)46:3<382::AID-JBM11>3.0.CO;2-R
- [15] S. Prasong, S. Yaowalak, S. Wilaiwan: *Pak. J. Bio. Sci.* 12(11) (2009) 872. DOI:10.3923/pjbs.2009.872.876
- [16] R. Ahmed, A. Kamra, S.E. Hasnain: *DNA Cell Biol.* 23(3) (2004) 149. PMID:15068584; DOI:10.1089/104454904322964742
- [17] K. Sen, K. Muruges Babu: *J. App. Poly. Sci.* 92 (2004) 1080. DOI:10.1002/app.13609
- [18] M. Li, W. Tao, S. Lu, C. Zhao: *Polym. Adv. Technol.* 19 (2008) 207. DOI:10.1002/pat.1018
- [19] H.W. Ouyang, J.C.H. Toh Siew Lok Goh, A. Thambyah, S.H. Teoh, E.H Lee: *Tissue Eng.* 9 (2003) 431. PMID:12857411; DOI:10.1089/107632703322066615
- [20] B.-M. Min, G. Lee, S.H. Kim, Y.S. Nam, T.S. Le, W.H. Park: *Biomaterials* 25 (2004) 1289. DOI:10.1016/j.biomaterials.2003.08.045
- [21] J. Sanchez-Ramos, S. Song, F. Cardozo-Pelaez, C. Hazzi, T. Stedeford, A. Willing, T.B. Freeman, S. Saporta, W. Janssen, N. Patel, D.R. Cooper, P.R. Sanberg: *Exp. Neurol.* 164(2) (2000) 247. PMID:10915564; DOI:10.1006/exnr.2000.7389
- [22] R. Quarto, G. Bianchi, A. Derubeis, M. Mastrogiacomio, A. Murgli, R. Cancedda: *Euro Cells Mat.* 4(1) (2000) 28.
- [23] A. Muthumanickam, E. Elankavi, R. Gayathri, Kubera S. Sampathkumar, G. Vijayakumar, K. Muthukumar, S. Subramanian: *Int. J. Mater. Res.* 12 (2010) 1548. DOI:10.3139/146.110429
- [24] N. Amiralayan, M. Nouri, M. Haghighat Kish: *Polymer Sci. Series, A* 52(4) (2010) 407. DOI:10.1134/S0965545X10040097
- [25] K. Frost, D. Kaminski, G. Kirwan, E. Lascaris, R. Shanks: *Carbohydrate Polym.* 78 (2009) 543. DOI:10.1016/j.carbpol.2009.05.018
- [26] K. Whang, K.E. Healy, D.R. Elenz, E.K. Nam, D.C. Tsai, C.H. Thomas, G.W. Nuber, F.H. Glorieux, R. Travers, S.M. Sprague: *Tissue Eng.* 5(1) (1999) 35. PMID:10207188; DOI:10.1089/ten.1999.5.35
- [27] S.G. Kumbar, R. James, S.P. Nukavarapu, C.T. Laurencin: *Biomed. Mater.* 3(3) (2008) 1. PMID:18689924; DOI:10.1088/1748-6041/3/3/034002
- [28] G. Freddi, P. Monti, M. Nagura, Y. Gotoh, M. Tsukada: *Poly. Phys.* 35 (1997) 841. DOI:10.1002/(SICI)1099-0488(19970415)35:5<841::AID-POLB13>3.0.CO;2-A
- [29] H.Y. Kweon, I.C. Um, Y.H. Park: *Polymer* 41 (2000) 7361. DOI:10.1016/S0032-3861(00)00100-2
- [30] H.Y. Kweon, I.C. Um, Y.H. Park: *Polymer* 42 (2001) 6651. DOI:10.1016/S0032-3861(01)00104-5
- [31] W.U. Huawen, Th. Huser, A. Parikh, V. Yeh: *Asia Optical Fiber Communication and Optoelectronic Exposition and Conference (AOE)* (2008).
- [32] M.Z. Li, W. Tao, S. Kuga, Y. Nishiyama: *Poly. Adv. Technol.* 1 (2003) 694. DOI:10.1002/pat.409
- [33] T. Asakura, C. Tanaka, M. Yang, J. Yao, M. Kurokawa: *Biomaterials* 25 (2004) 617. DOI:10.1016/S0142-9612(03)00570-2

(Received January 31, 2012; accepted August 27, 2012; online since November 14, 2012)

## Bibliography

DOI 10.3139/146.110888  
*Int. J. Mater. Res. (formerly Z. Metallkd.)*  
 104 (2013) 5; page 498–506  
 © Carl Hanser Verlag GmbH & Co. KG  
 ISSN 1862-5282

## Correspondence address

Dr. S. Subramanian  
 Associate Professor  
 Department of Textile Technology  
 Anna University Chennai  
 Tamil Nadu  
 Chennai -600 025  
 India  
 Tel.: 91-44-22359247  
 E-mail: ssresgroup12@gmail.com

You will find the article and additional material by entering the document number **MK110888** on our website at [www.ijmr.de](http://www.ijmr.de)